Studies of photo-induced protein reactions by spectrally silent reaction dynamics detection methods: Applications to the photoreaction of the LOV2 domain of Phototropin 1 from *Arabidopsis Thaliana*

Masahide Terazima

Department of Chemistry, Graduate School of Science, Kyoto University, Kyoto 606-8502, Japan

FAX: +81-75-753-4026

e-mail: mterazima@kuchem.kyoto-u.ac.jp

key words: protein reaction, diffusion, dynamics, photosensor

Summary

Biological function involves a series of chemical reactions of biological molecules, and during these reactions, there are numerous spectrally silent dynamic events that cannot be monitored by absorption or emission spectroscopic techniques. Such spectrally silent dynamics include changes in conformation, intermolecular interactions (hydrogen bonding, hydrophobic interactions), inter-protein interactions (oligomer formation, dissociation reactions) and conformational fluctuations. These events might be associated with biological function. To understand the molecular mechanisms of reactions, time-resolved detection of such dynamics is essential. Recently, it has been shown that time-resolved detection of the refractive index is a powerful tool for measuring dynamic events. This technique is complementary to optical absorption detection methods and the signal contains many unique properties, which are difficult to obtain by other methods. The advantages and methods for signal analyses are described in detail in this review. A typical example of an application of time-resolved refractive index change detection is given in the second part: The photoreaction of the LOV2 domain of a blue-light photoreceptor from *Arabidopsis Thaliana* (phototropin 1).

1. Introduction

At the molecular level, biological function consists of a series of many chemical reactions of biological molecules. For understanding the molecular mechanisms of protein reactions, extensive and intensive efforts have been made in a variety of fields. In particular, it is well recognized that structural information is important and X-ray crystallographic data has been extensively accumulated. However, to understand biological functions, not only the static structure but also information on dynamics is essential because chemical reactions are dynamic in nature.

The reaction may contain changes in conformation, in intermolecular interactions (hydrogen bonding, hydrophobic interactions), in inter-protein interactions (oligomer formation, dissociation reaction) and in conformational fluctuations [1]. Because time-resolved detection is essential for revealing such dynamic properties, a variety of techniques have been developed. For example, time-resolved absorption detects over various frequency regions; UV/Vis, IR, NMR, and EPR have been developed and applied to many reaction systems. There is no doubt that the most frequently used techniques are absorption and emission detections in the UV/visible region [2, 3]. These are powerful techniques because of the applicability in a wide time range (femtosecond – days) and the high sensitivity. By using the optical transition of a probe molecule located in a protein, the change in the optical absorption enables us to trace dynamics with a spatial resolution at the molecular scale. This high spatial resolution should be a huge advantage, but, on the other hand, it also represents a potential disadvantage of this method; i.e., absorption change reflects only changes near a probe molecule and any spectrally silent dynamics occurring within the biological macromolecules are usually not observed. (Absorption spectroscopy in the IR region may detect conformation changes without a probe molecule. However, because of strong IR absorption by water, detection of

inter-protein interaction and time-resolved detection are still limited, if not impossible. In this article, we use a term of "the spectrally silent dynamics" for referring dynamics without spectral change in the UV/Vis region.)

There are three important spectrally silent dynamics in protein reactions. First, conformational changes are always crucial steps associated with the function of biomolecules. Catalytic activities or signal transduction processes generally accompany changes in the secondary, tertiary, or quaternary structure [1]. If these changes occur distal from the chromophore, it is quite difficult to detect the changes in dynamics. Second, intermolecular interactions including protein-protein, domain-domain, protein-water, are essential for function. Although there have been a number of techniques developed such as the surface plasmon resonance method, affinity chromatography, or size exclusion chromatography [2], detection of such events in the time domain has been quite difficult. Protein association and/or dissociation represent one of the key reactions involved in regulating molecular processes relating to a variety of biological functions, such as, gene transcription, signal reception or signal transduction [1]. Although association or dissociation reactions for small molecules with a UV-visible absorption can be monitored, and the kinetics of such reactions have been traced using transient absorption spectroscopy [4], the absorption spectra of chromoproteins that have much higher molecular masses are rather insensitive to the association/dissociation processes. In such cases, detection of these reactions is difficult, and this is particularly apparent when such reactions are transient. Some spectroscopic techniques such as tryptophane fluorescence detection may sometimes be applicable to detect such changes. However, if the location of the tryptophane moiety is far from the association or dissociation region, the emission may not change. Third, energetic and conformational fluctuations have been recently recognized to be very important factors in facilitating

the various, efficient reactions of biomolecules [5]. However, techniques to detect such fluctuations during the reaction processes have not matured yet. Therefore, although many spectrally silent processes could be involved in reactions between the initial triggering and biological function (Fig. 1), detection of such processes has remained quite difficult.

In this review, I describe our recent studies of chemical reactions of biological proteins using the time-resolved detection method of the refractive index. This technique is complementary to the optical absorption detection methods and the signal contains information on spectrally silent dynamics. Such dynamics have unique properties, which are difficult to obtain by other methods. The advantages and the signal analysis methods are presented.

The refractive index reflects a variety of properties of the solution (Fig. 2 [6]). In a time region in which many large amplitude motions of proteins appear (nanoseconds – seconds), there are three important contributions to the refractive index change (δn); the thermal energy (temperature change), volume change and absorption change. Because most conformational change of a protein always accompanies a change in volume, this detection method is powerful in monitoring the dynamics of the conformation change during most reactions. Furthermore, the temperature dependence and pressure dependence of the volume change represents the change in the thermal expansion volume and in the compressibility, respectively. These properties are related to the conformation fluctuations through the thermodynamic relationship [7]. The temperature dependence of the enthalpy change represents the change in the heat capacity. This quantity is related to the energy fluctuation [7] and also with the solvent exposed area of hydrophobic groups. It has been quite difficult or almost impossible to measure these quantities in the time domain by other traditional methods. Using the refractive index detection approach, it is possible to resolve time domain events.

We primarily use the pulsed laser-induced transient grating (TG) method to monitor the refractive index change over a wide time range [8]. Besides high sensitivity and high time-resolution, the TG method also enables the detection of the translational diffusion value. Using this method, we have successfully measured the time dependence of the diffusion coefficient (*D*), and found that *D* is exquisitely sensitive to changes in protein conformation. Hence, this time-resolved diffusion method is also powerful in detecting the spectrally silent dynamics. (Since proteins are large molecule, any single detection method cannot clarify everything in the reaction. For understanding reaction mechanism, it is apparent that one needs structural information using optical spectroscopy (near, mid and far IR), EPR, NMR and so on. The TG method presented in this review will be one piece of essential information for these studies.) This technique has been widely applied in many chemical reactions of biological proteins such as PYP [9-11], Phytochrome [12], YcgF [13], rhodopsins [14-17], AppA [18], PixD [19] and phototropins [20-24]. Not only applicable to photosensors, this method is applicable to investigations on the ligand dissociation reaction of myoglobin [25, 26], or protein folding reactions [27-29]. In this review, phototropins are taken as an example to demonstrate the merits of the TG method and to show what information can be obtained. In particular, we focus on the time-resolved measurement of the diffusion coefficient to determine the molecular events that occur during a photochemical reaction.

2. Information from the TG signal

For the measurement of the TG signal, a sample is photoexcited by an optical interference pattern between two pulsed laser beams [8, 30, 31] (Fig. 3). The photoexcitation by the interference pattern creates a sinusoidal modulation in the refractive index (*n*) and the absorption (*k*). The created refractive index and/or absorption gratings are monitored by the diffraction of a continuous wave

probe beam. For a thick grating, which is defined by a grating having a longer optical length than the grating fringe length, the probe beam is applied at an appropriate angle to satisfy the phase-matching condition (Bragg condition) [8]. In the case of weak diffraction, the grating intensity (I_{TG}) is approximately proportional to the square of the amplitude of the modulation in the refractive index (δn) and absorption (δk) :

$$I_{TG} \cong \alpha(\delta n)^2 + \beta(\delta k)^2 \quad (1)$$

where α and β are constants that represent the sensitivity of the system. Because the absorption term δk provides essentially the same information as the transient absorption method at the probe wavelength, only the refractive index term δn is considered in this review. Experimentally, the absorption term δk in the TG signal can be neglected using a non-resonant probe wavelength.

The refractive index change in this review mainly consists of the following three components.

1. After the nonradiative transition of the excited states, the temperature of the sample is raised by the released energy, and the density of the matrix is altered by the heating effect, which creates the thermal grating (δn_{th}). Amplitude of this contribution is proportional to the amount of the thermal energy released by the sample. By subtracting this amount from the absorbed photon energy, the enthalpy change (ΔH) of the molecule can be determined. The decay rate of this component is determined by the thermal diffusion process, such that the rate constant is given by $D_{th}q^2$ (D_{th}: thermal diffusivity, and q is the grating wavenumber).

2. The refractive index change may be induced by a molecular polarizability difference between the reactant and product molecules because of a change in the absorption spectrum. This contribution is called the population grating term. The population grating is related to the change in the absorption spectrum by the Kramers-Kronig relation. This signal component reflects the absorption spectrum

change not only close to the probe wavelength, but also changes at other wavelengths.

3. The density change caused by the reaction volume change gives rise to the volume grating. Because any conformation change of a macromolecule as well as solvation change results in a molar volume change, this component should be useful for detecting spectrally silent conformational changes and solvation changes. The magnitude of the volume change can be determined from the amplitude of this component.

The sum of the population and volume grating component is called the species grating. When the signal simultaneously consists of the thermal and species contributions, these contributions should be separated for quantitative measurements. The identification and separation can be accomplished using the characteristic decay rate of the thermal contribution, $D_{th}q^2$ [30, 31].

After the photochemical reaction upon the light irradiation of the grating pattern occurs, concentrations of the reactant and the product molecules are sinusoidally modulated and this modulation of the concentration produces the grating signal (Fig. 3). Because this concentration modulation gradually disappears due to translational diffusion processes, the time-profile of the TG signal should also depend on the molecular diffusion rate. If all chemical reactions are completed before the observation time of the signal, the TG signal may be expressed by

$$I_{TG}(t) = \alpha\{\delta n_{th}\exp(-D_{th}q^2t) + \Sigma\delta n_P\exp(-D_Pq^2t) - \Sigma\delta n_R\exp(-D_Rq^2t)\}^2 \qquad (2)$$

where the subscripts P and R stand for the product and the reactant, respectively, and $\delta n_{P(R)}$ is the peak-to-null refractive index difference at $t = 0$. The negative sign for δn_R represents the 180° phase shift of the fringe pattern versus that of the product because of the consumption of the reactant. Because D_{th} is generally much larger (ca. more than two orders of magnitude in a typical case) than $D_{P(R)}$ in solution [30-33], the thermal component can be separated from the species grating signal by

the time-resolved manner.

Because the diffusion coefficient is a useful property to measure conformational changes, we describe this property in more detail below.

3. Diffusion coefficient

The diffusion coefficient, *D*, is a physical property that represents the rate of molecular diffusion. The Stokes-Einstein relationship (Eq. (3)) is frequently used as a basis of the molecular interpretation of *D* [33],

$$D = k_B T / a \eta r \qquad (3)$$

where k_B, T, η, a and r are the Boltzmann constant, temperature, viscosity, a constant representing the boundary condition between the diffusing molecule and the solvent, and the radius of the molecule, respectively. On the basis of this equation, observed changes in *D* during the reaction have been frequently interpreted in terms of changes in the radius of the solute, i.e., volume change. This interpretation may be correct, if the oligomerization (or dissociation reaction) reaction takes place. In the case of dimerization, the molecular volume increases by two, so that the radius of the solute increases by the cubic square of 2; i.e., 1.26, and we expect *D* to decrease by a factor of 1.26. However, in the absence of such an oligomerization (or dissociation) reaction, the molecular volume of the protein will not change as much. Even for a large conformational change, e.g., a protein unfolding reaction, the partial molar volume may change by less than 20 cm^3/mol [34], which represents only ~0.2% of the total volume of a rather small protein. Even if the protein volume changes by 10% during the reaction, which is an unrealistically large change, *D* is expected to change by only 3%. Therefore, in general, the volume effect can be neglected unless an oligomerization or dissociation reaction takes place.

Another intuitive interpretation of a change in *D* may be a change in the shape of the macromolecule. *D* of a molecule with a non-spherical shape has been theoretically derived [33]. For example, the ratio of D of a prolate molecule (D_{prl}) which has a semimajor axis *a* and a minor axis *b*, to D of a spherical molecule (D_0) which has the same volume, is expressed as

$$\frac{D_{prl}}{D_0} = \frac{\ln[P + (P^2 - 1)^{1/2}]}{P^{-1/3}(P^2 - 1)^{1/2}}$$

as a function of $P=a/b$. The equation shows that the value of *D* is rather insensitive to the molecular shape. For example, if the shape of a molecule changes from a sphere to an elongated shape, *D* is expected to decrease. However, *D* only decreases by 4% when a protein reaction changes the protein shape such that the radius of the molecule along the semi-major axis is two times longer than the radius along the minor axis. Therefore, the effect of a molecular shape change on *D* is negligible. Considering the above estimation, one may expect that *D* is a rather insensitive property for measuring a change in protein conformation.

However, on the contrary to this expectation, large changes in *D* during chemical reactions have been frequently observed [9-24]. The exact origin of the change in *D* in some cases is currently unclear. However, one of the factors giving rise to the observed changes in *D* could be the changes in the intermolecular interactions. The intermolecular interaction between the molecule and the solvent affects the friction of the molecular movement in solution. A clear example has been reported for chemical reactions of aromatic molecules [35, 36]. *D* values of organic radicals were found to be much smaller than those of electronically closed shell molecules with similar sizes and shapes. This change was attributed to the enhanced intermolecular interactions between the radicals and solvent molecules. A relationship between *D* and the conformation of proteins (or polymers) has been

investigated previously. For example, it has been reported that *D* decreases significantly by the unfolding of myoglobin (Mb) [37] or cytochrome c (Cyt c) [27]. The change has been explained as follows. The secondary structures of the native Mb and Cyt c are mostly composed of α-helices, which are formed by intramolecular hydrogen bonding. On the other hand, the intermolecular hydrogen bonding between the protein and water molecules should be dominant for the unfolded conformation. This intermolecular interaction acts as friction for the translational movement and therefore leads to a reduction in *D*. Therefore, it may be reasonable to consider that the cause of the reduction in *D* is the unfolding of the α-helices or β-sheets of proteins. The hydrodynamic flow change, due to the conformation change, may be another simultaneously important factor, as shown below. The change of the intermolecular interaction can be considered as a change in the boundary condition of the Stokes-Einstein relation.

On the basis of the above consideration, although *D* has sometimes been expressed in terms of the hydrodynamic radius, such a term is a rather misleading term to describe the change in *D*. The "hydrodynamic radius" is not a molecular radius such as the "radius of gyration," which clearly defines the molecular physical size. The hydrodynamic radius has just the same meaning as *D*, as long as the Stokes–Einstein relation holds. Therefore, *D* is useful as a comparative term as long as corrections for viscosity and/or temperature are taken into account, and it should not be considered to represent the "radius" of a molecule.

Another argument is related to the surface corrugation and roughness of globular proteins. Using molecular dynamics simulations, the magnitude of structural fluctuations and the diffusion coefficient were shown to vary with the size of solvent molecules, and this result correlates with the correlation dimensions of the protein [38]. The correlation dimension D_2 is a parameter describing

the surface roughness of globular protein molecules, which is dependent on the size of a guest molecule approaching the protein. The larger D_2 is, the smaller the diffusion coefficient is. Based on this consideration, a smaller *D* indicates that the surface is rougher. This surface roughness may be considered to represent a looser structure.

One of advantages of the TG method is the high sensitivity towards the detection of *D*, and therefore the method is sensitive to molecular changes during chemical reactions. Even though the accuracy of the absolute value of *D* may not be high (e.g., in particular when D of the reactant and the product is close, the ambiguity of the fitting could be about ±10% error), the difference in *D* between the reactant and the product can be detected very sensitively. This high sensitivity comes from the fact that the signal reflects the *D*-change of only the photoexcited molecules. This point is in contrast with other techniques that measure diffusion such as light scattering or NMR methods. These traditional methods detect the diffusion of all molecules present in the solution. Hence, if the reaction yield is low, the signal is a mixture of the reacted and non-reacted species, which decreases the sensitivity to detecting a change in *D*. On the other hand, as shown later, the TG signal shows very prominent features when *D* changes. Even if there is a 5% change in *D*, it gives rise to a strong characteristic TG signal.

4. Time dependence of *D*

Besides the high sensitivity, another unique advantage of the TG method is a high time resolution for the *D* measurement. Previously, this advantage was demonstrated for studying *D* of unstable transient molecules [35, 36]. However, not only this method can determine *D* of short-lived species, it is now possible to measure the time development of *D*. Because *D* depends on the conformation of macromolecules, the time evolution of *D* represents the dynamics of the conformation change.

Hence, this method is a very powerful and useful approach for studying spectrally silent dynamics.

To obtain kinetic information from the signal, the TG signal representing the diffusion (diffusion signal) should be analyzed based on a proper model. However, because the time dependence of the TG signal reflects a variety of reaction dynamics as well as the diffusion process, it is sometimes difficult to judge whether the observed signal shows the time-dependent D or it is just reaction kinetics without a time dependent change in D. We have proposed three criterions to show the temporal changes in D [12-24].

First, to identify the diffusion signal, the rate constant of the signal profile should depend on q^2. However, as long as both D_P and D_R are time independent, the diffusion peak intensity should not depend on q^2 as predicted from Eq. (2). On the contrary, a clear indication of the time dependent D is a significant q^2 dependence of the diffusion peak intensity. The following feature was frequently observed; the TG signal in a fast time scale (i.e., with a large q^2) is weak and the intensity increased by increasing the observation time and decreasing q^2. This time dependence of the signal intensity can be explained in terms of the time dependent apparent D as follows. On the basis of Eq. (2), the signal intensity should be weak, when D_P is close to D_R, because of the cancellation of the two terms in Eq. (2). With an increase in the difference between D_P and D_R, the apparent signal intensity becomes stronger. Because D of the reactant (D_R) should be constant, the time dependent change in the signal intensity should come from the time-dependent change of D_P. (If there are several reactive states having different diffusion coefficients (D_R) and the equilibrium of the substates is slow, we should observe some phases having different D_R. Even in such a case, the time profile is expressed by a combination of Eq.(2) and the signal intensity shall not be time dependent. If the equilibrium of the substates is fast, they are averaged and we can observe only one component, e.g. Eq.(2). In

between these limiting situations, D of the reactant could be changed in the observation time range, but we should notice this change by analyzing the signals at various q, because the reactant and the product give rise to signals having opposite signs of the δn.)

Second, the time profile of the signal should show a drastic change that is dependent on q^2. Suppose the protein reaction proceeds uni-molecularly. In this case, the TG signal can show at most two different diffusion coefficients; the reactant and the product. If the profile cannot be fitted by the bi-exponential function, this fact indicates that the reaction cannot be a simple transformation from the reactant to the product, but an intermediate species is involved.

Third, more clear evidence for the time-dependent D may be obtained by the q^2t plot of the signals. When the profile in this time range reflects only the diffusion process with a constant D, temporal profiles of the TG signals can be expressed by a combination of terms of $\exp(-Dq^2t)$ (e.g., Eq. (2)). In this case, all the TG signals measured at various q^2 should have an identical shape when they are plotted against q^2t. On the other hand, if the profiles are not identical at the different q^2, the constant D cannot explain the observed TG profiles.

The observed diffusion signal should be analyzed using a proper model. Two typical reaction schemes are shown below as examples.

(i) Diffusion change in a time range of the diffusion signal:

$$R \xrightarrow{h\nu} I \xrightarrow{k} P$$

where R, I, P and k represent the reactant, the intermediate species, the final product and the rate constant of the change, respectively. In this case, the $\delta n_R(t)$ and $\delta n_P(t)$ are given by

$$\delta n_R(t) = \delta n_R \exp(-D_R q^2 t)$$

$$\delta n_P(t) = \left(\delta n_I - \frac{k}{(D_I - D_P)q^2 + k} \delta n_P \right) \exp\left(-(D_I q^2 + k)t\right) + \frac{k}{(D_I - D_P)q^2 + k} \delta n_P \exp(-D_P q^2 t)$$

(7)

where δn_I and D_I are the initial refractive index change due to the creation of the intermediate species and D of intermediate species, respectively.

(ii) Reverse reaction

$$R \xrightarrow{h\nu} P \xrightarrow{k} R$$

$$\delta n(t)=\delta n_1 \exp(-D_R q^2 t)+\delta n_2 \exp(-(D_P q^2+k)t) \quad (8)$$

where

$$\delta n_1 = -\delta n_R (D_P q^2 - D_R q^2)/(D_P q^2 - D_R q^2 + k)$$

$$\delta n_2 = \delta n_P - \delta n_R k/(D_P q^2 - D_R q^2 + k)$$

Similarly, a theoretical equation for other more complicated reactions can be derived rather easily.

5. Application to Phototropin reactions

For demonstrating the enormous potential of the TG method, and for showing the importance of spectrally silent dynamics in biological functions, studies on phototropins are presented in this review. Phototropin (phot) is a major member of the blue light receptors in plants. Phototropin proteins are involved in the photoregulation of phototropism, chloroplast relocations and stomatal opening [39-46]. In *Arabidopsis*, there are two types of phot, named phot1 and phot2, both of which have two LOV (Light-Oxygen-Voltage) domains (LOV1 and LOV2) in the N-terminal and a serine/threonine kinase domain in the C-terminal half, and a linker connecting the LOV2 and the kinase domains (Fig. 4). For light detection, phot1 and phot2 bind a flavin mononucleotide (FMN)

noncovalently as a chromophore in the LOV1 and LOV2 domains. LOV2 acts as the main molecular switch for the light regulation of the kinase. The studies on phot have been performed by many research groups [39-72].

Before describing the TG applications to the phototropin reactions, the reaction scheme obtained by studies using other techniques is briefly summarized. Primary processes during the photoreception of phot have been studied mainly by the transient absorption method [39-52]. Upon photoexcitation, the ground state of the LOV domains (D_{447}) is excited to the triplet state (L_{660}). In this state, the thiol group of a conserved cysteine in the LOV domains forms an adduct with the isoalloxazine ring in FMN (the S_{390} state) (Fig. 5). The information of this change in the chromophore should be transferred to the kinase domain to regulate the kinase activity. However, no absorption change was observed after this adduct formation, and the spectrum returned back to the original state in minutes.

Conformational changes in phot have been studied by X-ray crystallography of LOV2 of *Adiantum* phytochrome 3 as well as the crystallographic and Fourier transfer IR (FTIR) method for LOV1 of *Chlamydomonas* [54-57]. Both results showed only small conformational changes nearby the chromophore. In contrast, FTIR studies on the photoreaction in the LOV1 and the LOV2 domains of *Adiantum* phytochrome 3 in hydrated films detected conformational changes in the secondary structures of the backbone amino acid chains [58]. Furthermore, NMR and small-angle X-ray scattering studies reported conformational changes in the linker [59, 60]. However, there has been no kinetic study on the conformational changes before our TG measurements [20]. Hence, it was not clear whether or not the conformational changes accompanied the S_{390} state formation. Furthermore, is there another transient conformational change prior to the final conformation? In fact, by applying the TG method for detecting spectrally silent dynamics, it is now known that there are several

intermediates before the main conformational change.

5-1. Inter-protein interaction change of the Phot1LOV2 domain

(a) Photo-induced dimerization

The phot1LOV2 domain is a good example for demonstrating light regulation of the inter-protein interaction. The increase in the intermolecular interaction was shown to be due to the dimerization reaction [21]. The signal analysis of this conclusion is explained below. A typical example of the TG signal of a phot1LOV2 solution observed at 50 μM and at $q^2 = 3.4 \times 10^{10}$ m^{-2} is shown in Fig. 6. In order to extract information on the reaction dynamics from the signal, the TG signal should be decomposed into components of different origins and these origins should be identified. The first step in the assignment process is the measurement of the q^2 dependence. In this case, it was found that the initial decay-rise profile was expressed by a single exponential function and this time constant (1.9 μs) did not depend on q^2. The q^2-independence indicates that the dynamics represents a chemical reaction but not diffusion. Based on the results from the absorption detection, the 1.9 μs dynamics was attributed to the adduct formation process; from D_{447} to S_{390}. The major source of the signal comes from the population grating signal derived from the absorption change associated with the formation of the adduct.

The next component in the 100 μs time range was dependent on the q^2-value; the rate became faster with increasing q^2-value. This q^2-dependence indicates that these dynamics are characterized by the diffusion process. By comparing with the thermal grating signal of a calorimetric reference sample that should decay with a rate constant of $D_{th}q^2$, it was concluded that this decay was the thermal grating component created by the thermal energy due to the nonradiative transition from the excited state.

The TG signal appearing after this thermal grating signal was the species grating signal, which reflects the chemical reaction kinetics as well as the molecular diffusion process. Because the time range of this signal is dependent on the q^2-value, the kinetics should represent the molecular diffusion rate. The signal decayed to the baseline (70 ms in this figure) and then a rise-decay signal (diffusion peak) appeared. From this observation and that the negative sign of δn_{th}, the rise component corresponds to a negative change in the refractive index and the subsequent decay component to the positive change. By comparison with Eq. (2), the rise and decay components of the TG signal were attributed to the molecular diffusion processes of the reactant (ground state protein; (D_{447})) and the photo-product, respectively. The faster rate of the rising component than the rate of the decay indicates that the product diffuses slower than the reactant ($D_R > D_P$) in this time range.

The detection of the *D*-change and the kinetics was determined from the diffusion signal. Figure 7 depicts the q^2 dependence of the TG signal. It was found that the diffusion signal decayed to the baseline monotonously in a short time range (~ ms). This decay was expressed by a single exponential function. This single exponential decay in the ms time range clearly shows that *D* of the reactant (D_{447}) and the product (S_{390}) are the same ($D_R = D_P$); i.e., *D* does not change during the reaction in this observation time range. This fact suggests that phot1LOV2 does not change conformation significantly upon photoreaction within the time range of ~1 ms.

Previous studies of the LOV domain by NMR [59] and x-ray [55] measurements did not reveal significant changes in secondary structure, which is consistent with the above result. On the other hand, the conformation changes of the LOV domains of YtvA and phot from *Chlamydomonas reinhardtii* with the time constant of the adduct formation were reported by detecting the volume change [62, 69]. Furthermore, recent time-resolved IR experiment for the phot2LOV2-I403V mutant

showed an intermediate species as changes in secondary structure in the helix or loop region with a time constant of 120 μs [70]. It looks these results contradict with results by other techniques. However, we consider that these results are not inconsistent with the TG result (no diffusion change). As stated in Introduction, any local structural change (such as the adduct formation) leads the volume change, whereas the diffusion change occurs by more global change of the shape and/or changes in intermolecular interactions. (Such global conformation change has been sometime refereed as the diffusion sensitive conformation change (DSCC).) Hence, the volume change [62, 69] and the IR spectrum change without DSCC mean that the conformation change of the LOV domain by the adduct formation is a rather local change. Furthermore, the seeming discrepancy of the results between FT-IR and TG methods could be also explained, if the previously observed dynamics in FT-IR is due to the dimerization reaction as shown below. In millisecond time range, another intermediate was reported by the FT-IR measurement as changes in the secondary structure, including β-sheets [70]. This change was indeed observed as the volume change with a time constant of 9 ms by the TG method [23].

On the basis of the three criterions mentioned in Section 4, the origin of this q^2-dependent change was attributed to the time dependent D. The temporal profile of the TG signal was analyzed by a model with a time-dependent apparent D (Eq. (7)). By using the diffusion coefficient of the reactant $D_R = 9.8 \times 10^{-11}$ m^2/s (= D_I) and the product $D_P = 8.0 \times 10^{-11}$ m^2/s, the observed TG signal can be reproduced very well in a wide observation time range (i.e., at various q^2 values) using a single reaction rate, k. The time constant of the change determined from the fitting is 40 ms at 50 μM. Comparing D of phot1LOV2 (17 kDa, $D_R = 9.8\times10^{-11}$ m^2/s) with other water soluble proteins of similar size measured by different methods, it was concluded that phot1LOV2 exists in the

monomeric form in solution at this concentration.

There are two possibilities to explain the decrease in *D*; a conformational change and/or oligomerization. These different origins can be distinguished by the concentration dependence measurement. If the protein conformational change is responsible for the change in *D*, the reaction rate should be independent of concentration. On the other hand, if this *D*-change is caused by a multi-molecular process, the kinetics of the TG signal should be sensitive to the concentration. The TG measurement at various concentrations showed that the temporal profiles were dependent on the concentration [21]. This change was attributed to the concentration dependence of the rate of the D_P-change. In fact, it was shown that the *D*-change rate became slower at lower concentrations. This observation implied that more than one molecule is involved in the *D*-change process. Together with the 1.8 times increase in the molecular volume, it was concluded that dimerization is the cause of the *D*-change.

For producing the dimer, there may be two possible reaction schemes: the phototransformed phot1LOV2 (LOV*) is associated with the ground state phot1LOV2 (LOV) to yield a dimer (Scheme 1), or two phototransformed phot1-LOV2 form the dimer (Scheme 2).

Scheme 1 $\quad 2\,\mathrm{LOV} \xrightarrow{h\nu} \mathrm{LOV^*} + \mathrm{LOV} \xrightarrow{k_d} (\mathrm{LOV^*\text{-}LOV})$

Scheme 2 $\quad 2\,\mathrm{LOV} \xrightarrow{h\nu} 2\,\mathrm{LOV^*} \xrightarrow{k} (\mathrm{LOV^*})_2$

where k_d is a bimolecular reaction rate. These possibilities can be tested by measuring the laser power dependence of the rate constant, and it was found that Scheme 1 appropriately describes the dimerization process [21]. The bimolecular reaction rate k_d may be written as k_i[LOV], where k_i is the intrinsic bimolecular reaction rate constant and [LOV] is the concentration of phot1-LOV2. From the rate constant, k_i was found to be $6.6 \times 10^5\ \mathrm{M^{-1}\,s^{-1}}$. This value is much smaller than that of

the diffusion limited reaction rate calculated from D_R and the estimated reaction distance. This small k_i suggests that the dimerization reaction occurs only at a specific relative orientation of two phot1LOV2 monomers. The light-induced dimer should eventually dissociate to return back to the monomer in the dark state. Therefore, this dimer formation is not due to covalent bonding. This dimerization reaction itself may not be relevant with the biological reaction, because the longer protein phot1LOV2-linker exists as monomer and we did not observe dimerization reaction for this sample as described in 5-2. However, it could be also possible that the observed dimerization of the LOV domains plays an important role *in vivo*, specular to the PAS domains dimerization which has a regulative role. In this *in vitro* case, the light induced change in the protein-protein interaction (in more specific, dissociation reaction described below) may reflect the LOV- and linker- domains interaction (section 5-2), which should have physiological relevance.

(b) Photo-induced dissociation reaction

The dimerization reaction upon the photoexcitation of the monomer Phot1LOV2 indicates that the intermolecular interaction increases upon photoexcitation. After this finding, it was reported that [21], in the dark state, there exists a dimer species in solution, and the photoexcitation of the dimer induces a decrease in the intermolecular interaction. These findings were obtained by the following experiment and signal analysis. Figure 8 depicts the concentration dependence of the signal over a concentration range of 40–250 μM. When the concentration was low enough, the species grating signal decayed as a single exponential. This finding implies that this observation time window is faster than the dimer formation rate (i.e., no diffusion change). The signal showed the growth-decay feature when the concentration was increased (Fig. 8). This rise-decay profile is different from that observed in a slower time region (e.g., Figs. 6 or 7) in a sense that the signal did not reach the

baseline. The rise component is attributed to the diffusion of a product and the decay to that of the reactant. Apparently from the rates of the rise and decay components, one may easily find that the product diffusion is faster than that of the reactant at the high concentrations ($D_R < D_P$).

The signal was reproduced almost perfectly with $D_R = 8.0 \times 10^{-11}$ m^2/s, $D_I = D_R$, $D_P = 9.8 \times 10^{-11}$ m^2/s and $k^{-1} = 300$ μs. The D of the reactant and product agreed well with those of the dimer and monomer, respectively. Therefore, at these concentrated solutions, the reactant should exist in a dimeric form and the product as a monomer. The observed TG signal indicates that the dimer dissociates to yield the monomer with a time constant of 300 μs upon photoexcitation.

The light-induced monomer does not return back to the dimer in the dark state until the recovery of the chromophore. The findings in this and previous sections suggest that the light induced structural changes of the dimer and monomer could be different. The reaction scheme of Phot1LOV2 is summarized in Fig.9. This light induced dimerization and dissociation reactions cannot be detected by the vis/UV absorption spectrum so that they are completely spectral silent.

(c) Temperature dependence of the monomer-dimer equilibrium

The above result clearly showed that there are two species in the solution: monomer and dimer. Frequently, the monomer and dimer are in equilibrium and the equilibrium constant depends on temperature. Although the equilibrium of Phot1LOV2 was confirmed by an independent method, size exclusion chromatography [24], the equilibrium constant could not be determine by this traditional technique, because it was difficult to measure the absolute concentration due to the dilution effect. However, the temperature effect on the equilibrium constant was successfully determined by the TG method as follows.

The signals at various temperatures over the range of 278–303 K normalized by the concentration of

S_{390} were reported (Fig. 10). These signals indicated that the association reaction is the dominant source of the signal; i.e., the rise and decay components should represent the diffusion of the reactant (monomer) and the product (dimer), respectively. The relative intensity of the diffusion peak was found to decrease as the temperature decreased below 293 K. This temperature dependence was explained by the temperature dependence of the relative concentrations of the monomer and dimer as follows.

For the dimerization reaction of the monomer, the reactant is the monomer and the product is the dimer. Conversely, for the dissociation reaction, the reactant is the dimer and the product is the monomer. If both of these reactions are superimposed, these contributions cancel each other. The dominant signal at the high temperature represents the dimerization reaction. If the contribution of the dissociation reaction becomes larger, the signal intensity should decrease. From the analysis of the signal, the relative contribution was determined quantitatively. The equilibrium constant K between monomer and dimer was determined at various temperatures [24]. From the temperature dependence of K, the differences in the enthalpy (ΔH) and entropy (ΔS) between the monomer and dimer were determined to be 90 ± 10 kJ $(\text{mol/dimer})^{-1}$ and 307 ± 30 J $(\text{K mol/dimer})^{-1}$.

5-2. Phot1LOV2-linker

(a) Inter-domain interaction change

The TG technique revealed an inter-protein interaction change upon photoexcitation of Phot1LOV2. A description of how the above change in the inter-protein interaction is related with the domain-domain interaction change for a multi-domain sample, Phot1LOV2-linker, is presented below.

A typical example of the observed signal after photoexcitation of phot1LOV2-linker at a

concentration of 70 μM and at a grating wavenumber of $q^2 = 6.0 \times 10^{10}$ m^{-2} is shown in Fig. 11 [22]. This profile is qualitatively similar to that observed for phot1LOV2 without the linker, as explained above; i.e., the signal decayed to the baseline, and subsequently showed two rise-decay profiles before completely decaying to the baseline. Compared with the TG signal of Phot1LOV2, these phases were attributed to the adduct formation and the thermal diffusion. The time constant of the adduct formation was 2.0 μs, which is essentially identical to that of phot1LOV2 (i.e., 1.9 μs). This similarity between phot1-LOV2 and phot1LOV2-linker indicates that the linker part does not influence the kinetics of the photo-adduct formation. This result concurs with other data, as the linker is located distal from the chromophore binding site.

The rise and decay components of the TG signal after the thermal grating signal were attributed to the species grating because of the reactant and the product, respectively. The characteristic diffusion peak was explained in terms of the two different D values for the reactant and the product. Because the feature of the signal satisfied the three criterions for the time-dependent D, it was concluded that D_P is not constant in this time range but time-dependent. The observed TG signal was justified using Eq. (7), and $D_R = 9.2 \times 10^{-11}$ m^2/s and $D_P = 5.0 \times 10^{-11}$ m^2/s, with the time constant of the D-change equal to 1.0 ms.

In the previous Phot1LOV2 case, the change in D was attributed to the dimerization reaction. If we simply apply a similar consideration to this phot1-LOV2-linker case, the observed reduction of D_P by a factor of 1.84 compared with D_R indicates that the molecular volume increases by ~6.2 fold upon photoexcitation. Assuming that this volume increase is caused by the aggregation process, it is possible to postulate that about six molecules aggregate in the S state. However, contrary to the Phot1LOV1 case, the concentration dependence of the rate constant showed that these dynamics

should involve a unimolecular reaction. Therefore, the *D* change observed in the phot1LOV2-linker is not due to any aggregation process. Combining this consideration with the observation that the *D* value for the photo-product of the LOV2 domain does not change significantly, it was concluded that the conformational change in the linker region is the main cause of the *D* reduction. Based on the fact that *D* decreases considerably upon unfolding of the α-helices (as observed from the protein folding reaction studies [27-29]), it is reasonable to attribute the conformation change in the linker region to the unfolding of the α-helices. Indeed, this unfolding of the linker helix is consistent with the conclusions from the NMR spectroscopy [59, 60] and CD spectroscopy [63].

This TG kinetic measurement implies that the conformational change in the linker region does not accompany the formation of the S_{390} state (1.9 μs), because the time constant is much larger, i.e., 1.0 ms. This process is spectrally silent. Since we did not observe concentration dependence of the TG signal, we concluded that there is no contribution of the dimerization reaction between two LOV2 domains to the TG signal.

For revealing the reaction in more detail, the transient lens (TrL) method was used. The TrL method is another technique to monitor time dependence of the refractive index in a slower time region [73-75]. Information from the TrL signal is essentially the same as that from the TG signal. However, because the thermal diffusion process in the TrL method is much slower than that of the TG method [73-76], reaction dynamics in the sub-millisecond time region for the TrL signal is not superimposed by the kinetics of the thermal component. Consequently, any reaction kinetics (volume change) should be clearly observed. The TrL signal upon photoexcitation of phot1LOV2-linker was reported [22], and it showed the thermal lens component and other phases, which were attributed to the refractive index change because of a change in volume (volume lens component). The kinetics of

this volume change were fitted using a bi-exponential function with time constants of 300 μs and 1.1 ms. The sign of the refractive index changes was negative, indicating the molecular volume contracted during this process. The longer time constant, 1.1 ms, was very close to that of the *D* change detected by the TG measurement. Hence, this refractive index change should represent the dynamics associated with the unfolding of the α-helix. The volume contraction implies that the molecular volume of the α-helix is larger than that of the unfolded (probably random coil) conformation.

Interestingly, the faster rate, 300 μs, was quite similar to the rate of the photo-induced dissociation reaction of phot1LOV2 without the linker (Section 5-1(b)). When the linker part is absent, the phot1LOV2 domain forms dimer probably by hydrophobic interactions. When the linker part in the phot1LOV2-linker protein is associated with the LOV2 domain by a hydrophobic interaction before the unfolding of the linker region, it should dissociate from the LOV2 domain. Hence, it is reasonable to consider that the 300 μs-phase observed for the phot1LOV2-linker represents the dissociation process of the linker domain from the LOV2 domain. Therefore, following photoexcitation, the linker part dissociates from the LOV domain without the unfolding of the helices, and the linker part is then destabilized and finally unfolds with the time constant of 1 ms. This new state should be a precursor state of the T_{390} state and is called T_{390}^{pre}. The similar kinetics of the dissociation reactions of the dimer and phot1LOV2-linker suggests that the driving force of both reactions is the same; i.e., the photo-induced adduct formation between FMN and the Cys residue leads to a conformational change or change in protein fluctuation, which leads to the disruption of the hydrophobic association.

Figure 12 represents the photocyclic reaction scheme of phot1LOV2-linker determined by the

absorption monitoring and spectrally silent dynamics detection methods. It was found that the photoreaction of phot2LOV2-linker can be described by the same scheme [15].

(b) Temperature dependent reaction of phot1LOV2-linker

As shown in the previous section (Section 5-1(c)), the Phot1LOV2 dimer dissociates at high temperatures. Can the linker domain dissociate from the LOV2 core at high temperatures in a similar way? To answer this, the temperature dependence measurement of the TG signal of LOV2-linker was conducted [19]. Figure 13 shows the TG signal representing the molecular diffusion at various temperatures over the range of 278–303 K at relative low q^2 ($q^2 = 2.0 \times 10^{12}$ m^{-2}). The signal was normalized by the amount of the S_{390} state that had formed. The intensity of the diffusion peak was found to have increased with decreasing temperature. This tendency is opposite to what was observed for the LOV2 sample (Fig. 10). This temperature dependence was interpreted in terms of a decrease of the population of the reactant that contributes to the diffusion signal with increasing temperature; that is, there is an equilibrium between the reactive and the non-reactive structures in the dark state and the reactive state is energetically more stable. It is reasonable to consider that the photoexcitation of phot1LOV2 yields the blue shifted species (S_{390}) at any temperature; however, a part of the species did not induce a conformation change (T_{390}) at the higher temperatures.

As mentioned above, the origin of the *D*-change was attributed to the unfolding of helices in the linker region. Hence, although the photochemistry of the chromophore took place at any temperature, the conformational change in the linker was blocked for the non-reactive species. As a possible reason of the prohibited conformational change of the linker region, dissociation of the linker region from the phot1LOV2 domain at higher temperatures was suggested (Fig. 14). This dissociation of the linker region from the phot1LOV2 domain is consistent with an NMR study on *A. sativa*

phot1LOV2 with Jα-helix. According to this report, the dark adapted state is in an equilibrium between the LOV-Jα bound state and LOV-Jα dissociated state [71]. The presence of this equilibrium is consistent with the above conclusion from the TG method.

On the other hand, although the NMR study showed that the dissociated form resulted in the unfolding of the Jα-helix, the CD spectra at various temperatures did not show any apparent difference in shape and intensity [24]. One of possible origins of the different results between the CD and the NMR studies could be the difference in the samples: LOV2 with Jα-helix (404-560 aa of *A. Sativa* phot1) used in the NMR study, and LOV2 with linker for the above TG and CD study (449-661 aa of *Arabidopsis*). This difference may affect the protein structure. It is important to stress that the equilibrium is shown both by the TG and NMR methods. Recently, it was reported that appropriate mutations of the LOV domain (*A. sativa* phototropin) can stabilize the LOV-Jα association in the dark adapted state and this mutation should be useful for improving the engineering applications of the phototropins [72]. It may be quite interesting study for these mutants by the TG technique described above.

The observed temperature dependence might have a role in the phototropin protein biological functions. Many signal transduction mechanisms are dependent on temperature for maintaining their function over a wide range of physiological temperatures. Conversely, such signaling mechanisms are sensitive to changes in temperature. Phot1LOV2 was found to be a mixture of reactive and non-reactive species and the fraction of these species was dependent on the temperature. At the same time, the conformational change in phot1LOV2 should regulate biological function. On the basis of these facts, it was proposed that phot could be a temperature sensor in addition to being a photosensor. This postulate will require examination using *in vivo* systems.

6. Future perspectives

In this review, experimental methods to characterize reaction intermediates of proteins using the TG technique have been presented. In particular, the diffusion measurement in the time-domain has been the focus of the review. By measuring the time-profile and the signal intensity of the TG signal, spectrally hidden dynamics (dimerization, dissociation, domain-domain interactions and conformational changes) can be extracted by monitoring changes in the diffusion coefficient. This information is quite unique and no other method can extract such information. This method should be suitable to many other reaction systems, and therefore reveal hidden reaction mechanisms of proteins. I hope that this technique will be more frequently used method for studies of reactions of biological molecules in future, like CD, IR, or small angle X-ray scattering techniques.

Although the diffusion measurement was mainly described in this review, an important property that should be considered in the future could be the kinetics of the change in the fluctuation. Understanding the biological reactions at the molecular level represents a major target in many scientific fields, e.g., physical chemistry, biochemistry, medical science and engineering. A crucial factor in many of these reaction processes is "fluctuation". Biological molecules are always fluctuating due to thermal energy; even during reactions. Why can proteins perform selective and efficient reactions? Do molecular fluctuations have important roles in facilitating many reactions? Information on the static structures of the molecules represent a starting point, but additional information is crucially required to clarify the molecular mechanism working in huge thermal agitations and studies from a view point of fluctuation and reaction dynamics will be important.

In this respect, detection methods that accurately measure fluctuations are essential. Of course, several experimental techniques have been developed, such as single molecule spectroscopy, hole

burning, the photon echo, and so on. An important quantity that reflects protein fluctuation is thermodynamic quantity. For example, it is well established that protein compressibility (β_T) is related with volume fluctuations ($(\Delta V)^2$) by a relationship of [7]

$$(\Delta V)^2 = -k_B T\left(\frac{\partial V}{\partial P}\right)_T = k_B \beta_T VT$$

where P and V denote the pressure and molar volume, respectively. Hence, if the compressibility is traced along the reaction coordinate, it is possible to obtain information about changes in fluctuation during the reaction. Because the TG method can measure thermodynamic quantities in time domain, this type of method is valuable in extracting such dynamics. Although there has been no report on the compressibility measurement in time-domain yet due to the technical difficulty using high pressure, it will be reported in near future. Accumulation of data on protein fluctuations over the coming years will enable researchers to determine whether such fluctuations are enhanced during a reaction. Developing theoretical methods to characterize fluctuations is also a research target of this field.

Acknowledgments

A part of this study was supported by a Grant-in-Aid (No.13853002) from the Ministry of Education, Science, Sports and Culture in Japan. The author is deeply indebted to co-authors of the papers referenced in this Review, in particular, Dr.T.Eitoku, Dr.Y.nakasone, Dr. D.Matsuoka, and Prof.S.Tokutomi.

References

[1] D.L.Nelson, M.M.Cox, Lehninger principle of biochemistry, 3rd ed, Worth Pub.2000.

[2] K.E.van Holde, W.C.Johnson, P.S.Ho, Principle of physical biochemistry, Printice-Hall International, New Jersey, 1998.

[3] Fluorescence Spectroscopy in Biology, Ed. by M. Hof, R. Hutterer and V. Fidler, Springer, 2004.

[4] R.Torre, Time-Resolved Spectroscopy in Complex Liquids, Springer, 2007.

[5] T.Neusius, Thermal Fluctuations of Biomolecules, Sudwestdeutscher Verlag, 2009.

[6] M.Terazima, N.Hirota, S.E. Braslavsky, A.Mandelis, S.E.Bialkowski, G.J. Diebold, R. J. D. Miller, D. Fournier, R.A. Palmer, A.Tam, Quantities, terminology and symbols in photothermal and related spectroscopies, Pure Appl. Chem., 76, (2004) 1083–1118.

[7] L.D.Landau, E.M.Lifshitz, Statistical Physics, Pergamon, London, 1959.

[8] H.J.Eichler, P.Günter, D.W.Pohl, Laser-induced dynamic gratings, Springer-Verlag, Berlin, 1986.

[9] K.Takeshita, N.Hirota, Y.Imamoto, M.Kataoka, F.Tokunaga, M.Terazima, Temperature dependent volume change of initial step of the photoreaction of Photoactive Yellow Protein studied by the transient grating, *J.Am.Chem.Soc.*, 122, (2000) 8524-8528.

[10] J.S.Khan, Y.Imamoto, M.Kataoka, F.Tokunaga, M.Terazima, Time-resolved thermodynamics: Heat capacity change of transient species during photo-reaction of PYP, *J.Am.Chem.Soc.*, 128, (2006) 1002-1008.

[11] J.S.Khan, Y.Imamoto, M.Harigai, M.Kataoka, M.Terazima, Conformational changes of PYP monitored by diffusion coefficient: Effect of N-terminal α-helices, *Biophys.J.*, 90, (2006) 3686-3693.

[12] T.Eitoku, X.Zarate, G.V. Kozhukh, J.-I.Kim, P.-S. Song, M.Terazima,Time-resolved detection of

conformational changes in Oat Phytochrome A: Time-dependent diffusion, *Biophys.J.*, 91, (2006) 3797-3804.

[13] Y.Nakasone, T.Ono, A.Ishii, S.Masuda, M.Terazima, Transient dimerization and conformational change of a BLUF protein: YcgF, *J.Am.Chem.Soc.*, 129, (2007) 7028-7035.

[14] Y. Nishioku, M. Nakagawa, M. Tsuda, M.Terazima, Energetics and Volume Changes of the Intermediates in the Photolysis of Octopus Rhodopsin at a physiological temperature, *Biophy.J.*83, (2002) 1136-1146.

[15] Y. Nishioku, M. Nakagawa, M. Tsuda, M.Terazima, A spectrally silent transformation in the photolysis of octopus rhodopsin: a protein conformational change without any accompanying change of the chromophore's absorption., *Biophy.J.*,80, (2001) 2922-2927.

[16] K.Inoue, J.Sasaki, M. Morisaki, F.Tokunaga, M.Terazima, Time-resolved detection of the Sensory Rhodopsin II- Transducer interaction, *Biophys.J.*, 87, (2004) 2587-2597.

[17] K.Inoue, J.Sasaki, J.L. Spudich, M. Terazima, Laser-induced Transient Grating Analysis of Dynamics of Interaction between Sensory Rhodopsin II D75N and the HtrII Transducer, *Biophys.J.*, 92, (2007) 2028-2040.

[18] P.Hazra, K.Inoue, W. Laan, K.J. Hellingwerf, M.Terazima,Tetramer Formation Kinetics in the Signaling State of AppA monitored by the time-resolved diffusion, *Biophys.J.*, 91, (2006) 654-661.

[19] K.Tanaka, Y. Nakasone, K.Okajima, M. Ikeuchi, S. Tokutomi, M.Terazima,Oligomeric State-Dependent Conformational Change of a BLUF Protein TePixD (Tll0078), J.Mol.Biol., 386, (2009) 1290-1300.

[20] T.Eitoku, Y.Nakasone, D.Matsuoka, S.Tokutomi, M.Terazima,Conformational dynamics of Phototropin 2 LOV2 domain with the linker upon photoexcitation, *J.Am.Chem.Soc.*, 127, (2005)

13238-13244.

[21] Y.Nakasone, T.Eitoku, D.Matsuoka, S.Tokutomi, M.Terazima,Kinetic measurement of transient dimerization and dissociation reactions of *Arabidopsis* phototropin 1 LOV2 domain, *Biophys.J.*, 91, (2006) 645-653.

[22] Y.Nakasone, T.Eitoku, D.Matsuoka, S.Tokutomi, M.Terazima, Dynamics of conformational changes of Arabidopsis phototropin 1 LOV2 with the linker domain, *J.Mol.Biol.*, 367, (2007) 432-442.

[23] T. Eitoku, Y. Nakasone, K. Zikihara, D. Matsuoka, S.Tokutomi, M. Terazima,Photochemical intermediates of *Arabidopsis* phototropin 2 LOV domains associated with conformational changes, *J.Mol.Biol.*, 371, (2007) 1290-1303.

[24] Y. Nakasone, T. Eitoku, K. Zikihara, D. Matsuoka, S.Tokutomi, M. Terazima, Stability of dimer and domain-domain interaction of Arabidopsis phototropin 1 LOV2, J.Mol.Biol., 383, (2008) 904-913.

[25] M.Sakakura, S.Yamaguchi, N.Hirota, M.Terazima,Dynamics of structure and energy of horse carboxymyoglobin after photodissociation of the carbon monoxide, *J.Am.Chem.Soc.,* 123, (2001) 4286-4294.

[26] M.Sakakura, I.Morishima, M.Terazima, The structural dynamics and ligand releasing process after the photodissociation of sperm whale carboxymyoglobin, *J.Phys.Chem.*B,105, (2001) 10424-10434.

[27] T.Nada, M.Terazima,A novel method for study of protein folding kinetics by monitoring diffusion coefficient in time domain, *Biophys.J.*, 85, (2003) 1876-1881.

[28] S.Nishida, T.Nada, M.Terazima,Kinetics of intermolecular interaction during protein folding of

reduced cytochrome *c*, *Biophys.J.*, 87, (2004) 2663-2675.

[29] S.Hirota, Y.Fujimoto, J.Choi, N.Baden, N.Katagiri, M.Akiyama, R.Hulsker, M.Ubbink, T.Okajima, T.Takabe, N.Funasaki, Y. Watanabe, M.Terazima Conformational Changes during Apoplastocyanin Folding Observed by Photocleavable Modification and Transient Grating, *J.Am.Chem.Soc*., 128, (2006) 7551-7558.

[30] M. Terazima, Molecular volume and enthalpy changes associated with irreversible photo-reactions, J.Photochem.Photobiol.C, 3, (2002) 81-108.

[31] M. Terazima, Time-resolved thermodynamic properties of intermediate species during photochemical reactions, Bull. Chem. Soc. Jpn, 77, (2004) 23-41.

[32] CRC Handbook of Chemistry and Physics (91st), CRC Press, 2010.]

[33] E.L.Cussler, Diffusion, 2nd edition, Cambridge University Press, 1997.

[34] N. Baden, S. Hirota, T. Takabe, N. Funasaki, M. Terazima,Thermodynamical properties of reaction intermediates during apoplastocyanin folding in time-domain, *J.Chem.Phys.*, 127, (2007) 175103 (1-12).

[35] M.Terazima, N.Hirota, Translational diffusion of a transient radical studied by the transient grating method; pyrazinyl radical in 2-propanol, *J.Chem.Phys.*, 98, (1993) 6257-6262.

[36] M.Terazima, Translational diffusion of organic radicals in solution, *Acc.Chem.Res.*,33, (2000) 687-694.

[37] J.Choi, M.Terazima, Denaturation of a protein monitored by diffusion coefficients: Myoglobin, *J.Phys.Chem.B*, 106, (2002) 6587-6593.

[38] J-H. Choi, H.Kim, S.Lee, Correlation dimension as a measure of surface roughness of protein molecules, J.Chem.Phys., 109, (1998) 7001-7004.

[39] E. Huala, P. W. Oeller, E. Liscum, I. S. Han, E. Larsen, W. R. Briggs, Arabidopsis NPH1: a protein kinase with a putative redox-sensing domain. *Science*. 278, (1997) 2120-2123.

[40] W. R. Briggs, E. Huala, Blue-light photo-receptors in higher plants. *Annu. Rev. Cell Dev. Biol*. 15, (1999) 33-62.

[41] J. M. Christie, P. Reymond, G. K. Powell, P. Bernasconi, A. A. Raibekas, E. Liscum, et al., Arabidopsis NPH1: a flavoprotein with the properties of a photo-receptor for phototropism. *Science*. 282, (1998) 1698-1701.

[42] J. A. Jarriol, H. Gabrys, J. Capel, J. M. Alonso, J. R. Ecker, A. R. Cashmore, Phototropin-related NPL1 controls chloroplast relocation induces by blue light. *Nature*. 410, (2001) 952-954.

[43] T. Kinoshita, M. Doi, N. Suetsugu, T. Kagawa, M. Wada, K. Shimazaki, Phot1 and phot2 mediate blue light regulation of stomatal opening. *Nature*. 414, (2001) 656-660.

[44] M.Kimura, T.Kagawa, Phototropin and light-signaling in phototropism, Curr Opin Plant Biol., 9,(2006) 503-8.

[45] J.M.Christie, Phototropin blue-light receptors, Annu Rev Plant Biol. 58, (2007) 21-45.

[46] E. Demarsy, C.Fankhauser, Higher plants use LOV to perceive blue light, Curr. Opin. Plant Biol.,12, (2009) 69-74. and references therein.

[47] T. E. Swartz, S. B. Corchnoy, J. M. Christie, J. W. Lewis, I. Szundi, W. R. Briggs, R. A. Bogomolni, The photocycle of a flavin-binding domain of the blue light photoreceptor phototropin, *J. Biol. Chem.* 276, (2001) 33500–36493.

[48] T. Kottke, J. Heberle, D. Hehn, B. Dick, P. Hegemann, Phot LOV1: photocycle of a blue-light receptor domain from the green alga Chlamydomonas reinhardtii, *Biophys. J.* 84, (2003) 1192-1201.

[49] T. A. Schüttrigkeit, C. K. Kompa, M. Salomon, W. Rüdiger, M. E. Michel-Beyerle, Primary

photophysics of the FMN binding LOV2 domain of the plant blue light receptor phototropin of Avena sativa, *Chem. Phys.* 294, (2003) 501-508.

[50] J. T. M. Kennis, S. Crosson, M. Gauden, I. H. M. van Stokkum, K. Moffat, R. van Grondelle, Primary reactions of the LOV2 domain of phototropin, a plant blue-light photoreceptor, *Biochemistry.* 42, (2003) 3385-3392.

[51] E. Schleicher, R. M. Kowalczyk, C. W. M. Kay, P. Hegemann, A. Bacher, M. Fischer, R. Bittl, G. Richter, S. Weber, On the Reaction Mechanism of Adduct Formation in LOV Domains of the Plant Blue-Light Receptor Phototropin, *J. Am. Chem. Soc.* 126, (2004) 11067-11076.

[52] K. M.Folta, E. P.Spalding, Unexpected roles for cryptochrome 2 and phototropin revealed by high-resolution analysis of blue light-mediated hypocotyl growth inhibition, *Plant. J.* **26**, (2001) 471-478.

[53] R. Fedorov, I. Schlichting, E. Hartmann, T. Domratcheva, M. Fuhrmann, P. Hegemann, Crystal structures and molecular mechanism of a light-induced signaling switch: the Phot-LOV1 domain from Chlamydomonas reinhardtii, *Biophys. J.* 84, (2003) 2492-2501.

[54] S. Crosson and K. Moffat, Structure of a flavin-binding plant photoreceptor domain: insights into light-mediated signal transduction. *Proc. Natl. Acad. Sci. USA.*, 98 (2001) 2995-3000.

[55] S. Crosson, K. Moffat, Photoexcited structure of a plant photoreceptor domain reveals a light-driven molecular switch, *Plant Cell.*, 14 (2002) 1067-1075.

[56] T. E. Swartz, P. J. Wenzel, S. B. Corchnoy, W. R. Briggs, R. A. Bogomolni, Vibration spectroscopy reveals light-induced chromophore and protein structural changes in the LOV2 domain of the plant blue-light receptor phototropin 1, *Biochemistry.* 41 (2002) 7183-7189.

[57] R. Fedorov, I. Schlichting, E. Hartmann, T. Domratcheva, M. Fuhrmann, P. Hegemann., Crystal

structures and molecular mechanism of a light-induced signaling switch: the Phot-LOV1 domain from Chlamydomonas reinhardtii, *Biophys. J.*, 84 (2003) 2492-2501.

[58] T. Iwata, D. Nozaki, S. Tokutomi, H. Kandori, Comparative Investigation of the LOV1 and LOV2 Domains in Adiantum Phytochrome3, *Biochemistry*., 44 (2005) 7427-7434.

[59] S. M. Harper, L. C. Neil, K. H. Gardner., Structural Basis of a Phototropin Light Switch, *Science.*, 301 (2003) 1541-1544.

[60] S. M. Harper, J. Christie, K. H. Gardner, Disruption of the LOV-J Helix Interaction Activates Phototropin Kinase Activity, *Biochemistry,* 43 (2004) 16184-16192.

[61] M. Nakasako, T. Iwata, D. Matsuoka, S. Tokutomi, Light-Induced Structural Changes of LOV Domain-Containing Polypeptides from Arabidopsis Phototropin 1 and 2 Studied by Small-Angle X-ray Scattering, *Biochemistry.* 43 (2004) 14881-14890.

[62] A.Losi,T.Kottke, P.Hegemann, Recording of Blue Light-Induced Energy and Volume Changes within the Wild-Type and Mutated Phot-LOV1 Domain from Chlamydomonas reinhardtii, Biophys.J.,86, (2004) 1051-1060.

[63] S.B.Corchnoy, T.E.Swartz, J.W.Lewis, I.Szundi, W.R.Briggs, R.A.Bogomolni, Intramolecular Proton Transfers and Structural Changes during the Photocycle of the LOV2 Domain of Phototropin 1. *J. Biol. Chem.* **278**, (2003) 724-731.

[64] H.Guo, T. Kottke,P. Hegemann, B.Dick, The Phot LOV2 Domain and Its Interaction with LOV1, Biophys.J., 89, (2005) 402-412.

[65] M.T. Alexandre, T. Domratcheva, C.Bonetti, L.J.van Wilderen, R. van Grondelle, M.L.Groot, K.J. Hellingwerf, J.T. Kennis. Primary reactions of the LOV2 domain of phototropin studied with ultrafast mid-infrared spectroscopy and quantum chemistry, Biophys J. 2009 ;97:227-37.

[66] M. T. A. Alexandre, R. van Grondelle, K. J. Hellingwerf, J. T. M. Kennis, Conformational Heterogeneity and Propagation of Structural Changes in the LOV2/Ja Domain from Avena sativa Phototropin 1 as Recorded by Temperature-Dependent FTIR Spectroscopy, Biophys.J., 97 (2009) 238-247.

[67] T.Koyama, T. Iwata, A. Yamamoto, Y. Sato, D. Matsuoka, S. Tokutomi, H. Kandori, Different role of the Jalpha helix in the light-induced activation of the LOV2 domains in various phototropins, Biochemistry, 48,(2009) 7621-8.

[68] A.Pfeifer, T.Mathes, Y.Lu, P. Hegemann, T. Kottke, Blue light induces global and localized conformational changes in the kinase domain of full-length phototropin, Biochemistry, 49 (2010)1024-32.]

[69] A.Losi, B. Quest, W. Gärtner, Listening to the blue: the time-resolved thermodynamics of the bacterial blue-light receptor YtvA and its isolated LOV domain,Photochem.Photobiol.Aci., 2, (2003)759–766.

[70] A. Pfeifer, T.Majerus K. Zikihara, D. Matsuoka, S. Tokutomi, J. Heberle, T. Kottke, Time-resolved Fourier Transform Infrared study on photoadduct formation and secondary structural Changes within the phototropin LOV domain, Biophys.J., 96 (2009), 1462-1470.

[71] X.Yao, M. K Rosen, K. H. Gardner, Estimation of the available free energy in a LOV2-J alpha photoswitch. Nat. Chem. Biol. **4**, (2008), 491-497.

[72] D. Strickland, X. Yao, G. Gawlak, M. K. Rosen, K. H Gardner, T. R Sosnick, Rationally improving LOV domain–based photoswitches, Nat.Methods, 7 (2010), 623-626.

[73] M. Terazima, Energetic and molecular dynamics in solution studied by the third order nonlinear optical spectroscopies; Transient lens and transient grating, *Advances in multiphoton processes and*

spectroscopy,Eds.,S.H.Lin, A.A.Villaeys, Y.Fujimura, World Scientific,Singapore, Vol.10, (1996) 1-96.

[74] M.Terazima, Transient lens spectroscopy in a fast time scale, *Israel J. Chem.*, 38, (1998) 143-157.

[75] S.E.Bialkowski, Photothermal spectroscopy methods for chemical analysis, John-Wiley, 1996.

Figure captions

Fig. 1. A schematic illustration of a photosensor protein reaction to induce a biological response. Spectrally silent processes are key steps for understanding protein reactions and for determining the biological function of the macromolecule.

Fig. 2. A flow chart showing the causes of the refractive index change following photoexcitation of proteins in solution.

Fig. 3. (Upper) Schematic illustration of the TG method. (Lower) Concentration modulation induced by the grating light irradiation causes the creation of the TG signal. Open circles; reactant, closed circles; product. The grating wavenumber q is defined by $2\pi/\Lambda$, where Λ is the fringe length of the grating. The concentration modulation gradually decreases with time by the translational motion of the molecules so that the TG signal intensity decreases.

Fig. 4. Schematic showing the domains of phot. The light absorption of the chromophore in the LOV domains initiates the phot reaction and the light information is transferred to the kinase domain.

Fig. 5. Photoreaction of the chromophore of phot (FMN). The kinetics of this reaction can be monitored by an optical absorption detection method.

Fig. 6. A TG signal (broken line) of phot1LOV2 at $q^2 = 3.4 \times 10^{10}$ m^{-2} [16]. The best fitted curve to the observed TG signal by Eq. (7) is represented by the solid line. Assignments of the kinetics in the signal were labeled.

Fig. 7. The q^2 dependence of the diffusion signals (broken lines) of phot1LOV2 [16]. The arrow shows the increase of the q^2-value, which are 5.3×10^{12}, 6.3×10^{11}, 3.4×10^{11}, 7.3×10^{10} and 4.5×10^{10} m^{-2} following the curves from left to right. The best-fitted curves to the observed TG signals by

Eq. (7) are represented by the solid lines.

Fig. 8. Concentration dependence of the TG signals (broken lines) of phot1-LOV2 solutions in a short time region [16]. The arrow shows the increase in the concentration. The concentrations are 56, 110, 180, 200 and 300 μM from the lower to higher curves. The signals are normalized at the initial part of the diffusion signal. The best-fitted curves to the observed TG signals using Eq. (7) are represented by the solid lines. Assignments of the kinetics in the signal were labeled.

Fig. 9. Schematic showing the photoreaction process of phot1-LOV2 detected by TG, (a) light-induced dissociation of LOV2 dimer and (b) light-induced association of two LOV2 monomers.

Fig. 10. (a) Temperature dependence of the observed TG signal (gray broken lines) after photoexcitation of phot1LOV2 [19]. The temperatures were 303, 298, 293, 288, 283 and 278 K in the direction of the arrow. The best fitted curves using Eq. (7) are represented by the black solid lines.

Fig. 11. An example of the observed TG signal (dotted line) of Phot1LOV2-linker at $q^2 = 6.0 \times 10^{10}$ m^{-2} [17]. The best fitted curve using Eq. (7) is represented by the solid line.

Fig. 12. Photo-cyclic reaction of the phot1LOV2-linker including the spectroscopically active and silent dynamics. The color of the chromophore indicates the changes in the absorption spectra (blue: dark adapted state, red: excited triplet state, yellow: lit state). The equilibrium between the folded and unfolded forms of the linker both in the dark and in the light state (Fig.14) is also taken into account in this scheme.

Fig. 13. Temperature dependence of the observed TG signal (gray broken lines) after photoexcitation of the phot1LOV2-linker [19]. The temperatures were 278, 283, 288, 293, 298 and

303 K in the direction of the arrow. The best fitted curves using Eq. (7) are represented by the black sold line.

Fig. 14. Schematic illustration showing the analogy of the dimerization-dissociation equilibrium for phot1LOV2 and the linker association-dissociation equilibrium for the phot1LOV2-linker. Left figures represent a favorable conformation at higher temperature.

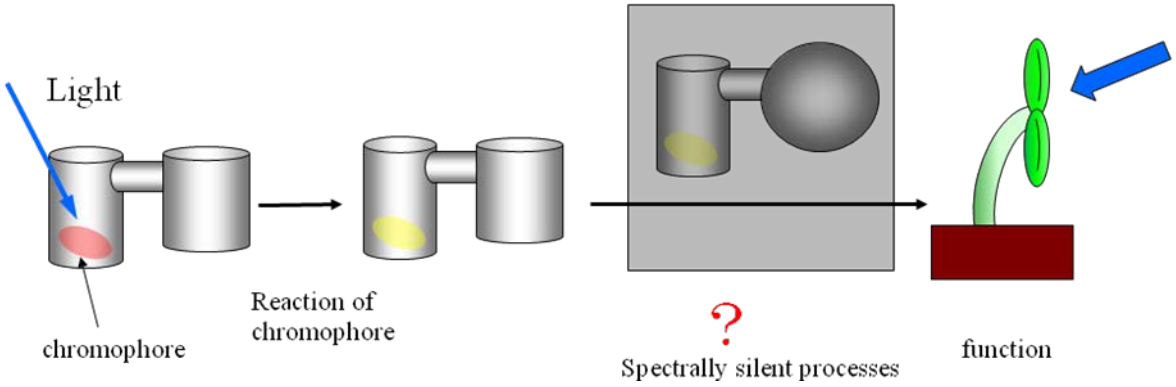
Light
chromophore
Reaction of
chromophore
?
Spectrally silent processes
function

Fig. 1

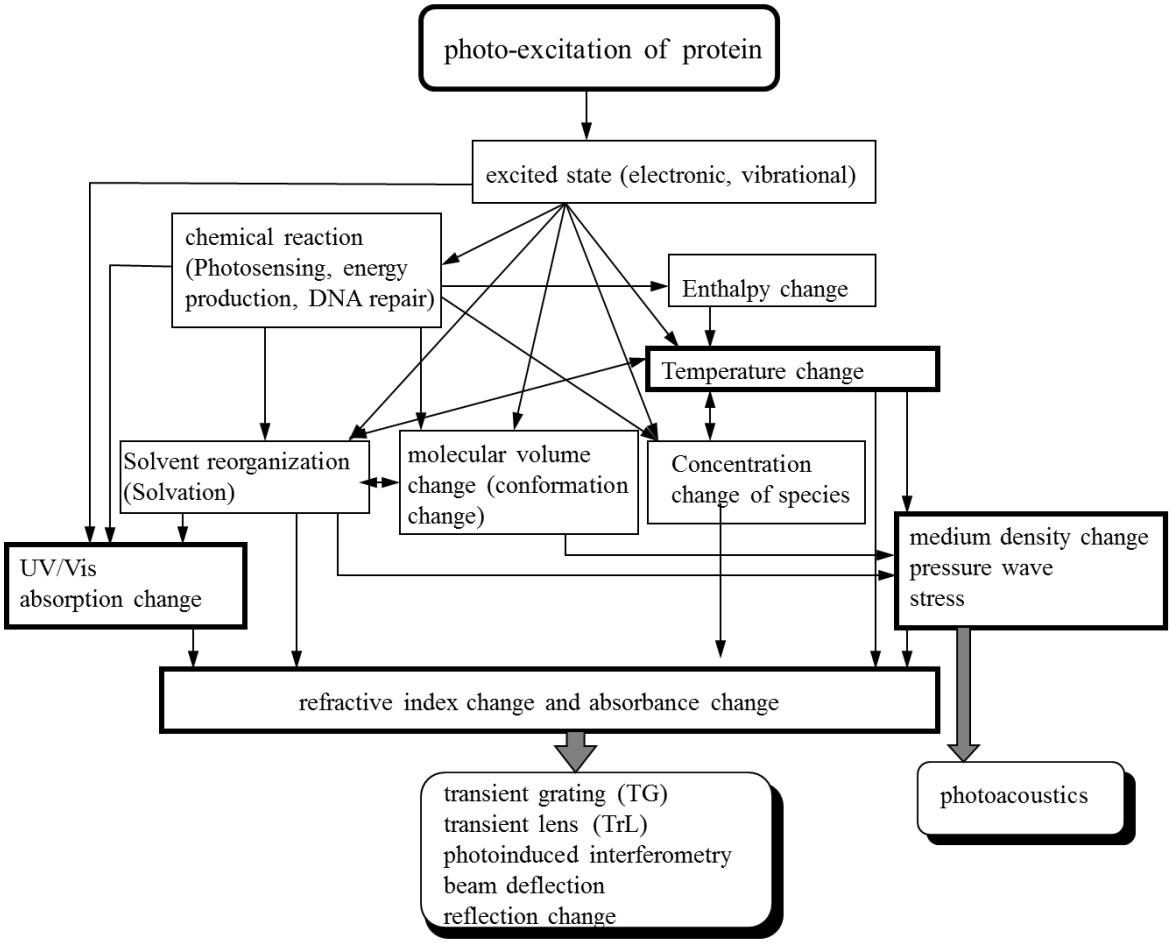
photo-excitation of protein
excited state (electronic, vibrational)
chemical reaction (Photosensing, energy production, DNA repair)
Enthalpy change
Temperature change
Solvent reorganization (Solvation)
molecular volume change (conformation change)
Concentration change of species
medium density change
pressure wave
stress
UV/Vis absorption change
refractive index change and absorbance change
transient grating (TG)
transient lens (TrL)
photoinduced interferometry
beam deflection
reflection change
photoacoustics

Fig. 2

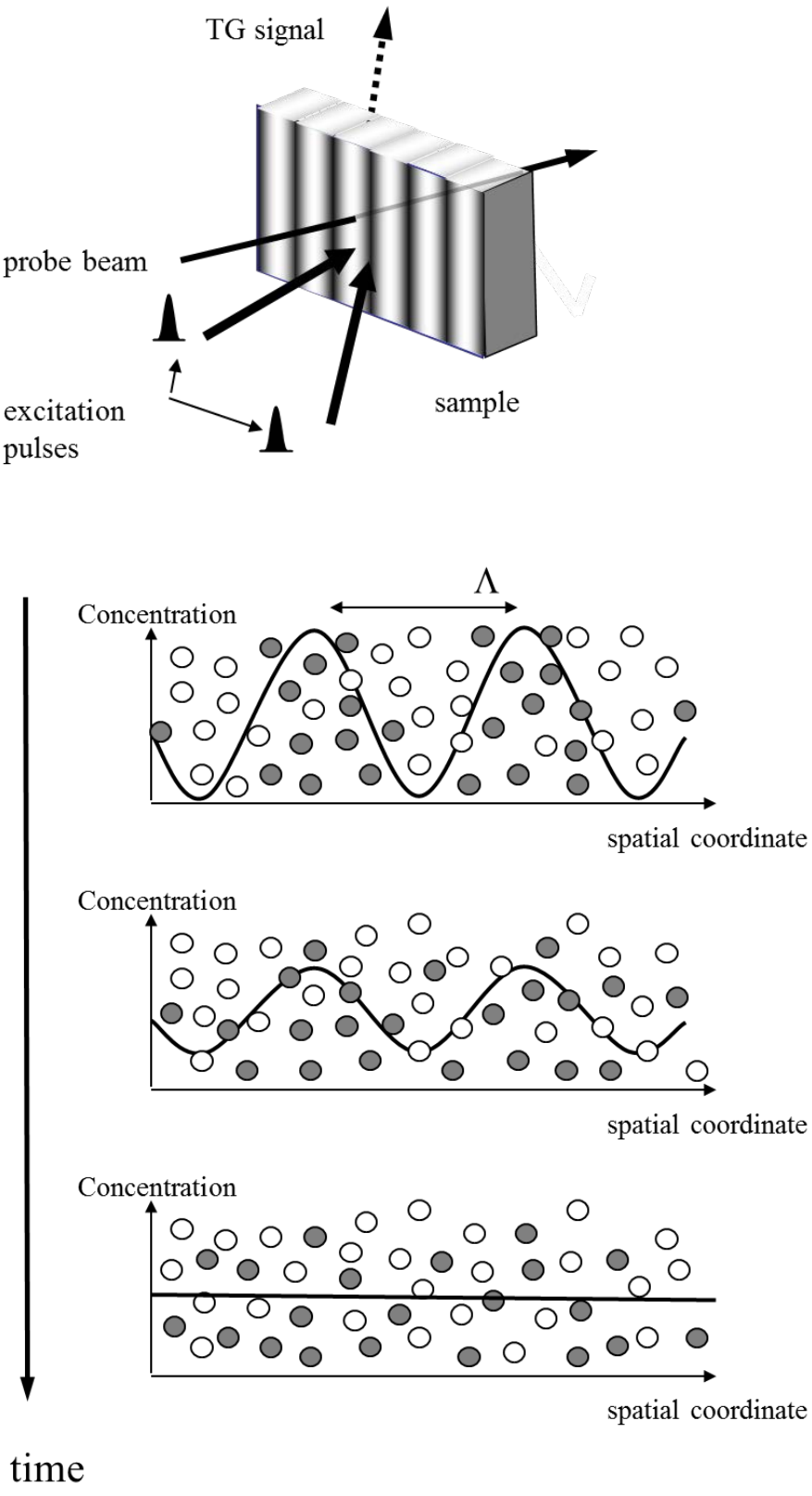
TG signal
probe beam
excitation
pulses
sample
Λ
Concentration
spatial coordinate
Concentration
spatial coordinate
Concentration
spatial coordinate
time

Fig. 3

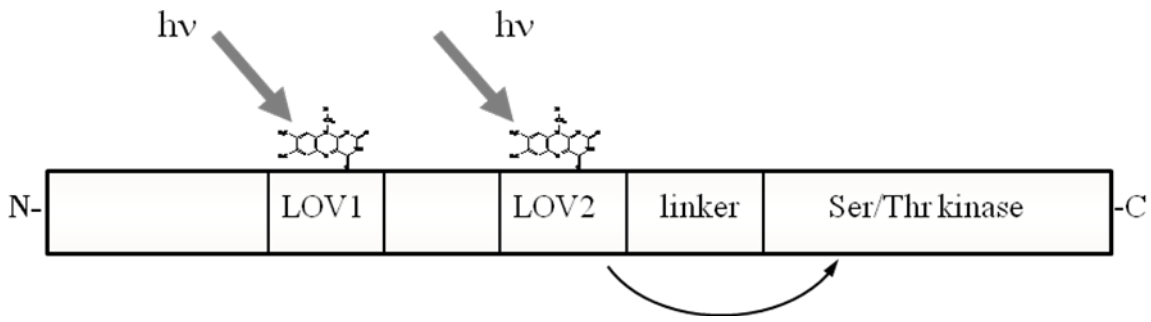

Fig. 4

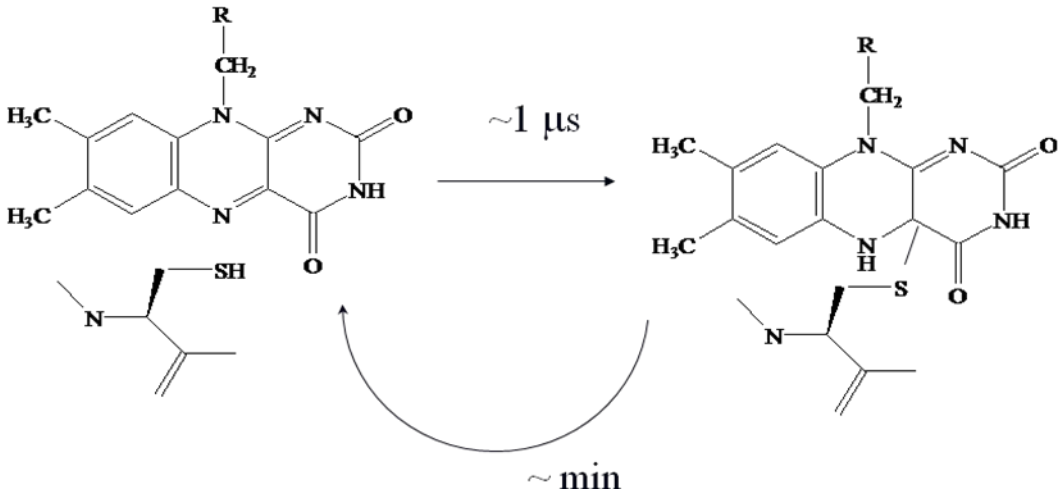

Fig. 5

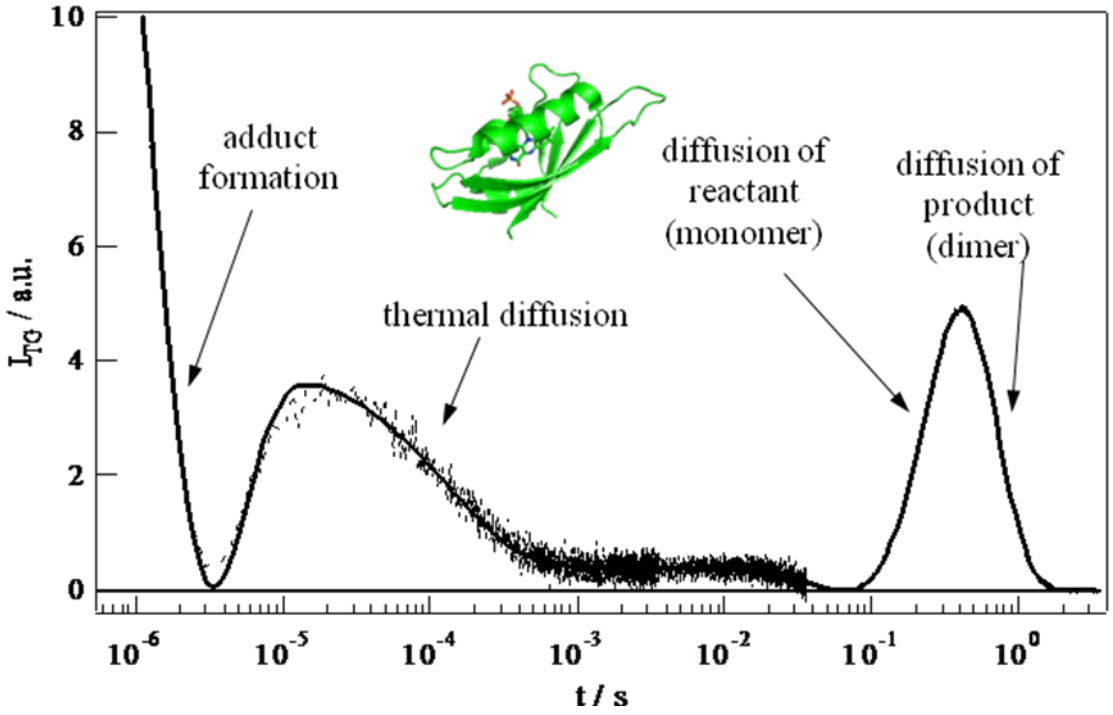
10
8
6
4
2
0
I_{TG} / a.u.
adduct
formation
thermal diffusion
diffusion of
reactant
(monomer)
diffusion of
product
(dimer)
10^{-6}
10^{-5}
10^{-4}
10^{-3}
10^{-2}
10^{-1}
10^{0}
t / s

Fig. 6

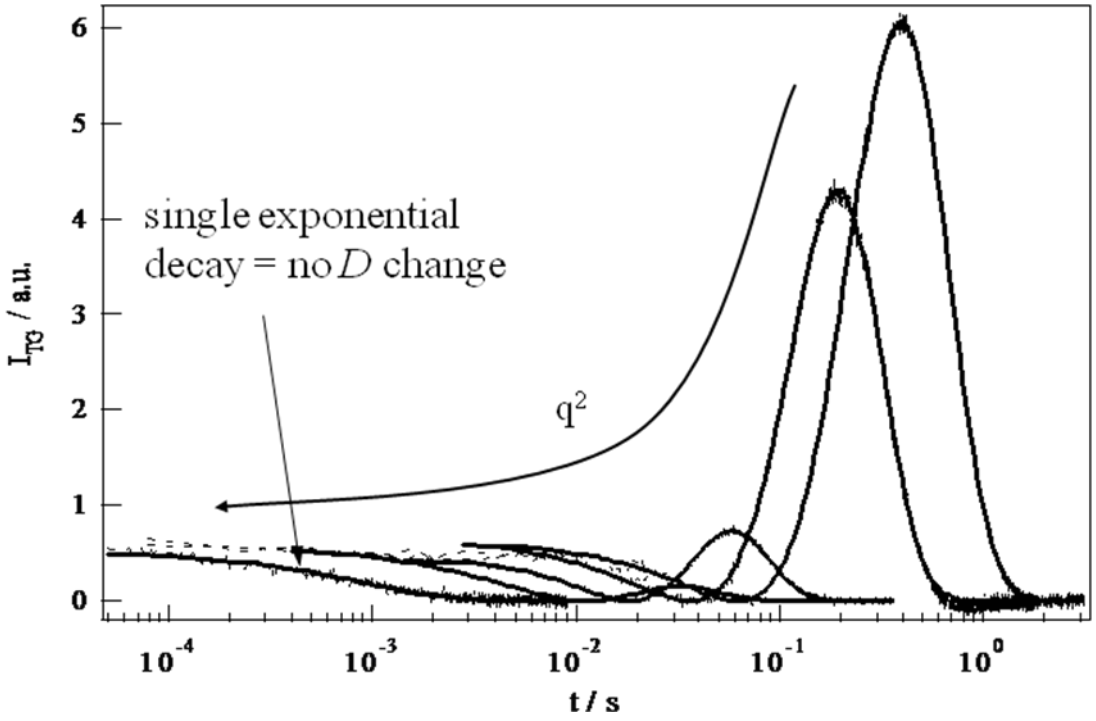
single exponential
decay = no D change
q²
I_PG / a.u.
t / s
0
1
2
3
4
5
6
10⁻⁴
10⁻³
10⁻²
10⁻¹
10⁰

Fig. 7

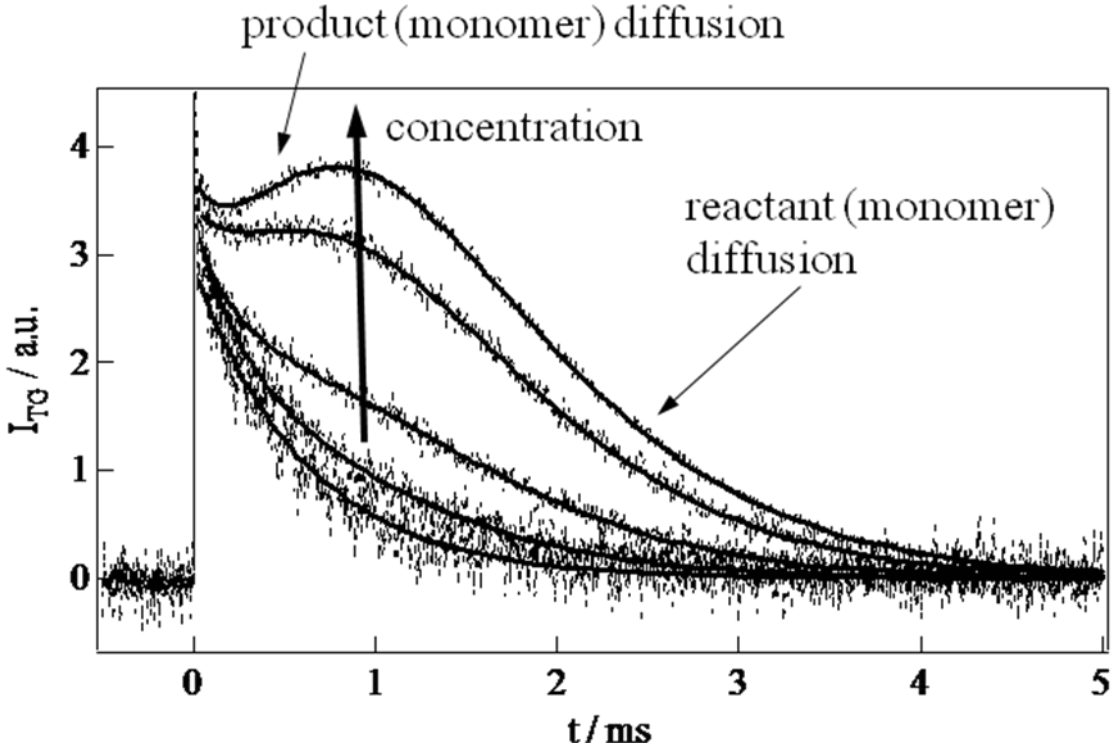
product (monomer) diffusion
concentration
reactant (monomer)
diffusion
I_{TG} / a.u.
t / ms
0
1
2
3
4
5

Fig. 8

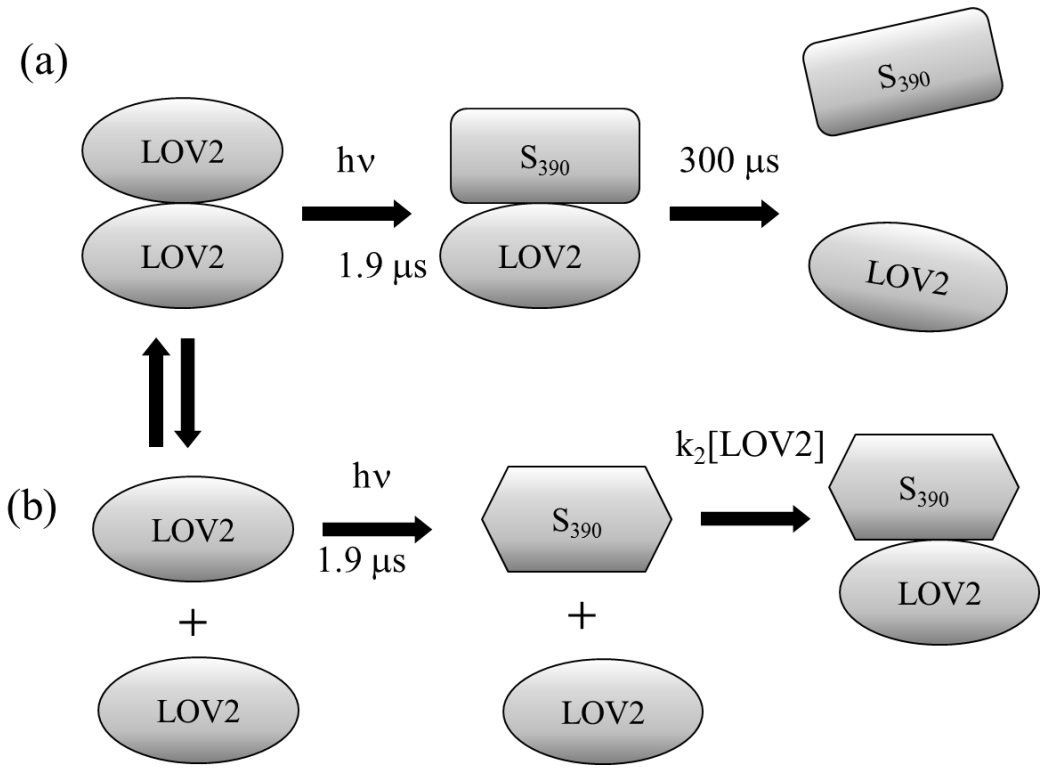
(a)
LOV2
LOV2
hν
1.9 μs
S390
LOV2
300 μs
S390
LOV2
(b)
LOV2
+
LOV2
hν
1.9 μs
S390
+
LOV2
k2[LOV2]
S390
LOV2

Fig. 9

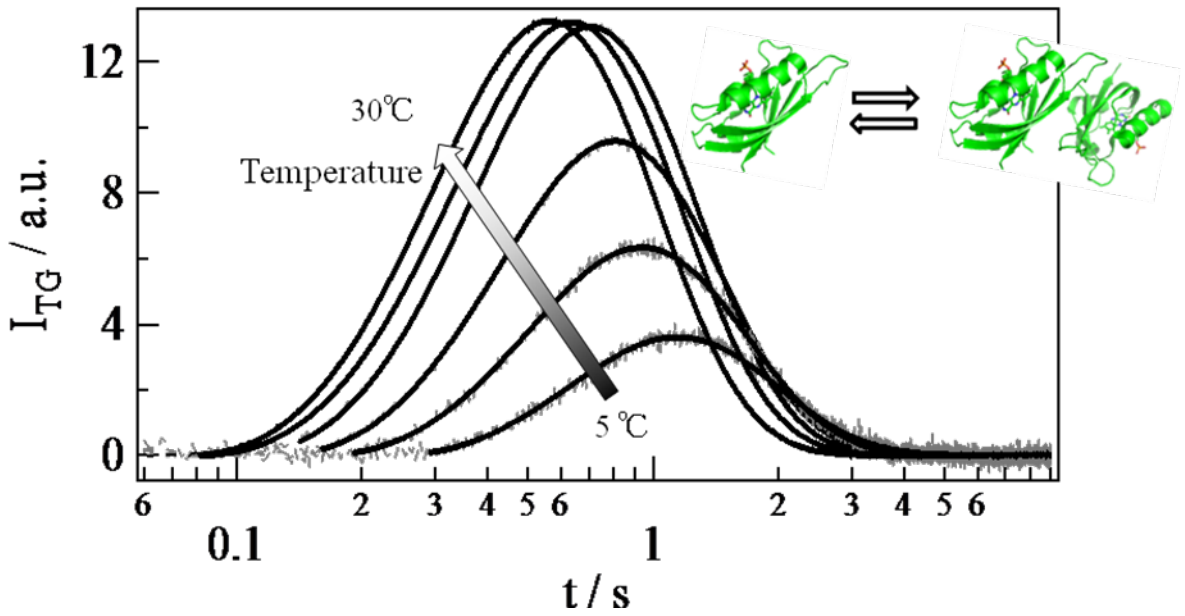

Fig. 10

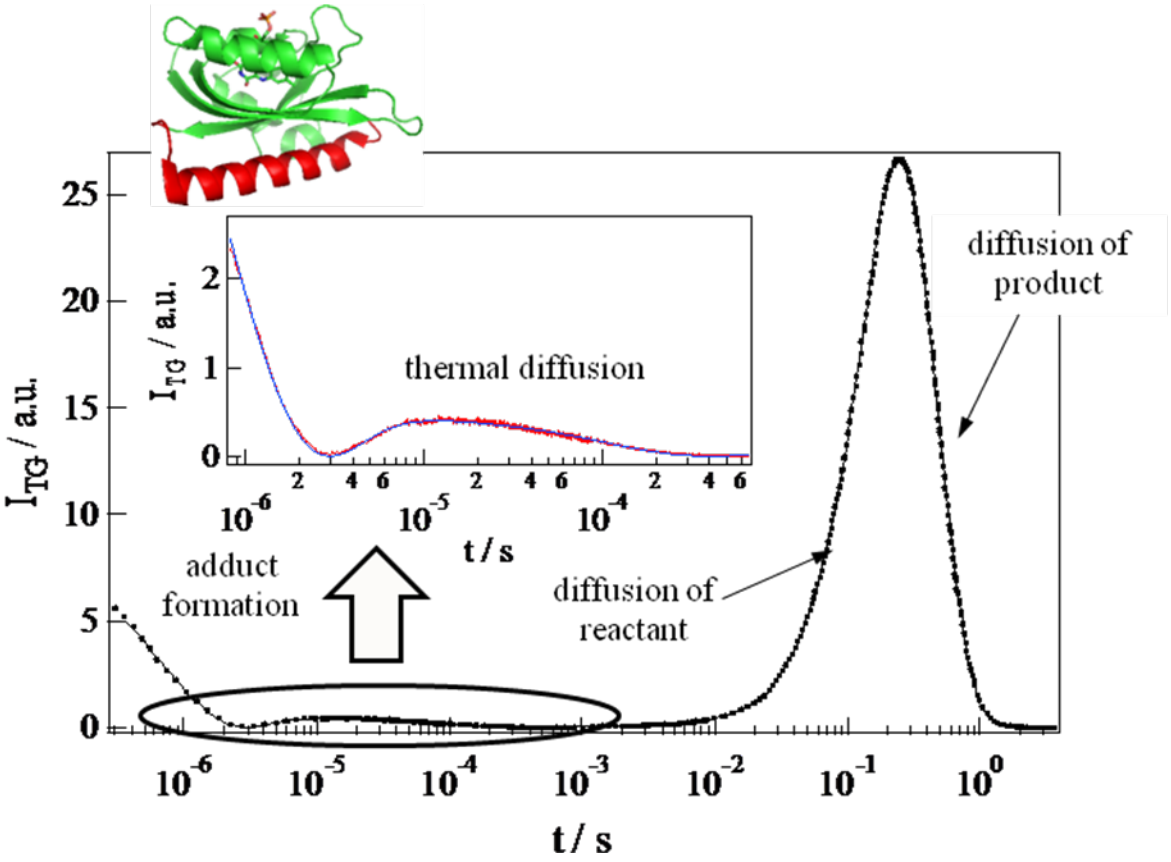
diffusion of product
thermal diffusion
adduct formation
diffusion of reactant
I_TG / a.u.
t / s

Fig. 11

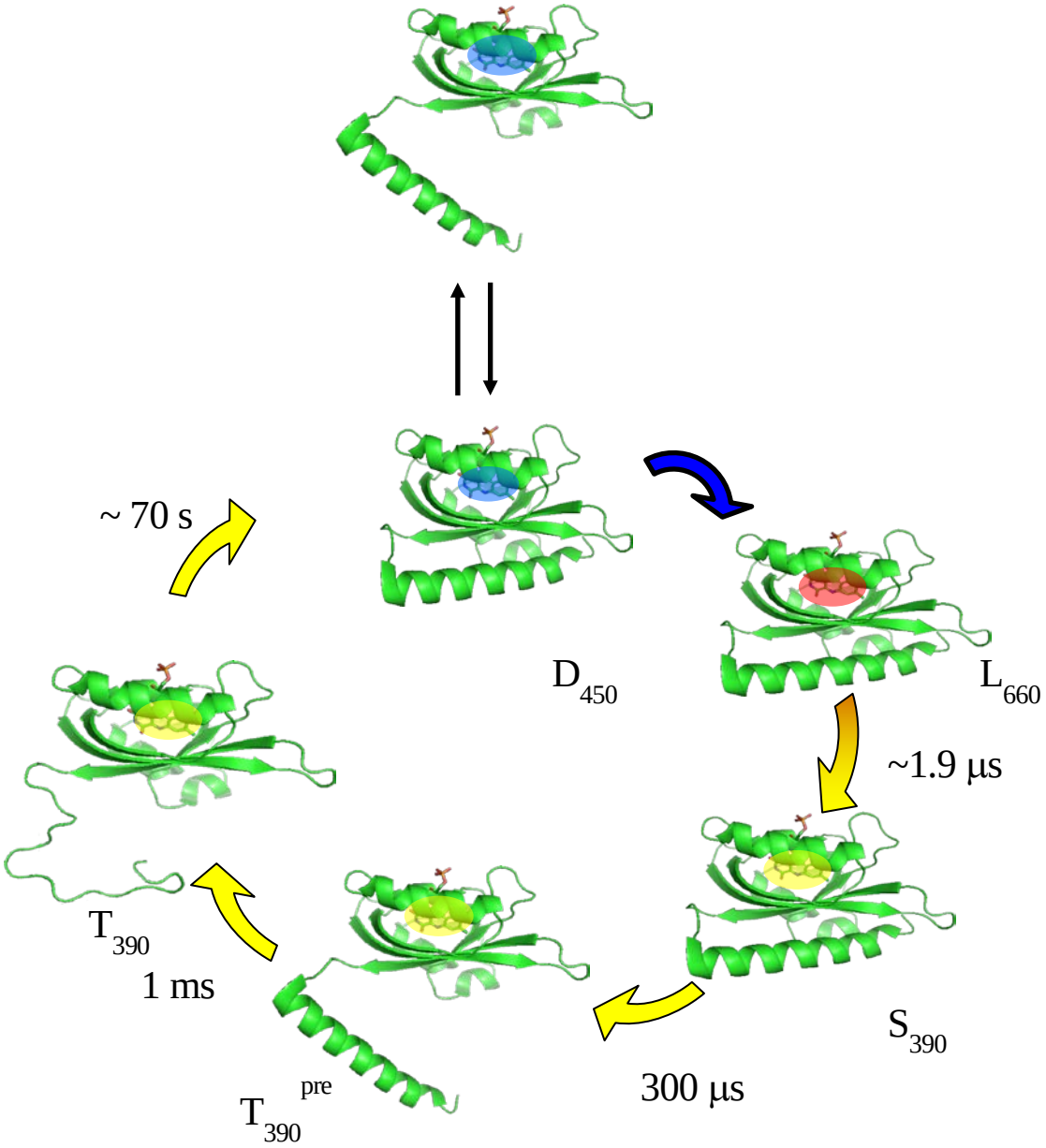

Fig. 12

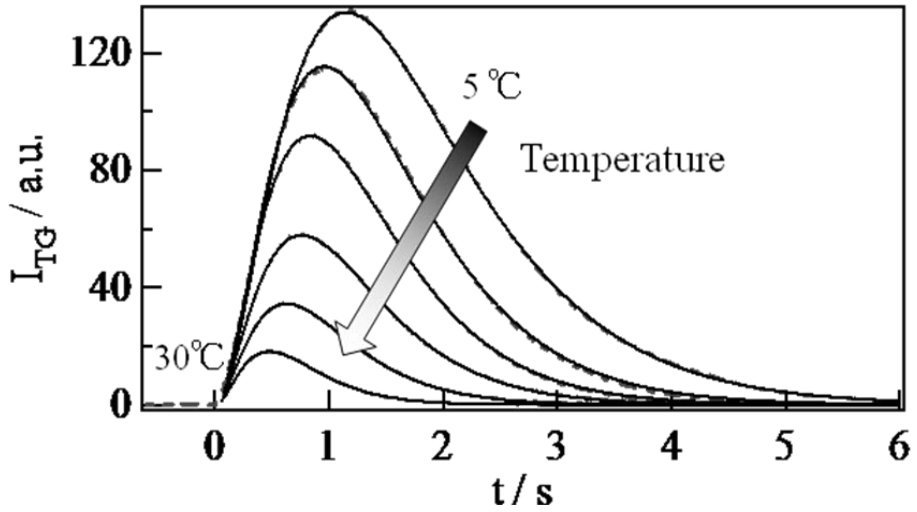

Fig. 13

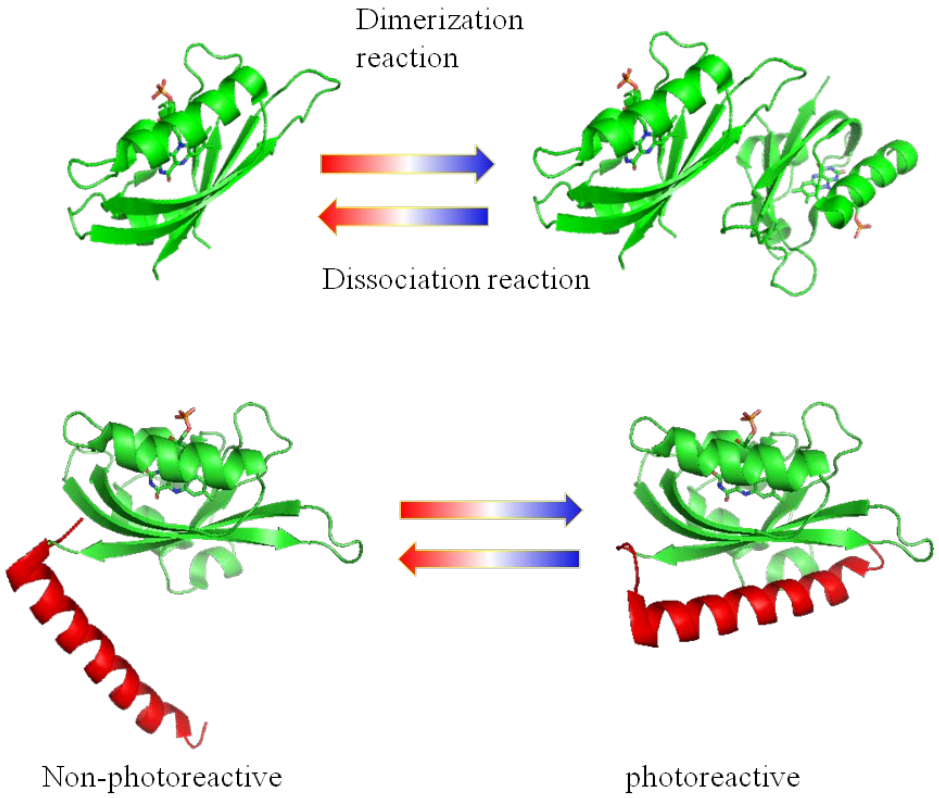
Dimerization
reaction
Dissociation reaction
Non-photoreactive
photoreactive

Fig. 14